The 9th European Congress on Computational Methods in Applied Sciences and Engineering
ECCOMAS Congress 2024
3–7 June 2024, Lisboa, Portugal

A DENSITY-BASED TOPOLOGY OPTIMISATION METHOD INCLUDING GEOMETRICAL UNCERTAINTIES

Florian Noal[1,*], Alain Etienne[1], Marco Montemurro[2], Jean-Yves Dantan[1] and Julien Gardan[3]

[1] Arts et Métiers Institute of Technology, Université de Lorraine, LCFC, 4 rue Augustin Fresnel, 57078 Metz Cedex 3, France, firstname.surname@ensam.eu

[2] Université de Bordeaux, Arts et Métiers Institute of Technology, CNRS, INRA, Bordeaux INP, I2M UMR 5295, F-33405 Talence, France, firstname.surname@ensam.eu

[3] Institut de Recherche, ESTP, 28 Avenue du Président Wilson, F-94230, Cachan, France, jgardan@estp.fr

Key words: Aleatory Uncertainty, Epistemic Uncertainty, Topology Optimisation, Design for Robustness, Additive Manufacturing

Summary. In the last decade, new topology optimisation (TO) algorithms have been proposed, with special features associated with Additive Manufacturing (AM) processes. However, AM is affected by a lack of repeatability: the integration of uncertainty is thus important. In this article, the integration of uncertainties that affect the part geometry in TO algorithms is considered. On the one hand, the proposed approach is based on a classic density-based TO algorithm. On the other hand, the uncertainty of geometrical features is handled through process-related variables. Furthermore, uncertainty characterisation of AM processes shows the need to integrate epistemic uncertainties as aleatory uncertainty. In this context, the mathematical framework related to uncertainty is based on *Dempster-Shafer* or *probability boxes* structures, instead of the classical probability one. The effectiveness of the approach is tested on various benchmark structures taken from the literature. Obtained geometries are consistent with the robust design approach, thanks to the integration of AM process-related variables into the topology optimisation process.

1 INTRODUCTION

Including information from the manufacturing process is crucial when considering generative design approaches, such as the Topology Optimisation (TO) algorithms. Process information can be included in different manners, but for one purpose: increase the performance of a product or a part. For instance, one can integrate the specificities of the process inside the optimisation procedure [18], in the spirit of the so-called Design for Manufacturing (DfM) approach. An alternative strategy consists of including information about the variability of the process, in order to design parts that are robust (or reliable) by taking into account the process deviations [11]: the resulting approach is often referred to as Design for Robustness (or Reliability) (DfR) approach. In this framework, two alternative design strategies can be considered: robust-based design or reliability-based design approaches. In the former, also called reliability-based optimisation, the designed part must meet its performance objective (despite uncertainties) over

a period of time. For this purpose failure probability should be estimated [16]. In the latter, unexpected behaviours of a part, under various uncertainty sources, are minimised [16]. It is worth noting that some cases in the literature are labelled as reliable, but they might be seen as robust design optimisation methodologies with probability constraints [16]. In robust design approaches, using statistical moments to optimise a design is a common practice. Regarding the reliability-based optimisation approaches, they allow determining optimised solutions in accordance with a prescribed probability of a failure event. In the following, only robust-based design methods will be considered, since the TO method presented in this paper belongs to this class.

Uncertainty sources of a physical system are the surroundings of the system, such as its boundary conditions or its main features, such as geometrical and material or physical properties, initial state, etc., [14]. Many works have been made in the context of Robust Topology Optimisation (RTO) by considering different uncertainty sources. For instance, material properties uncertainty was addressed in [11], representing the uncertainty of the Young's modulus through a Gaussian stochastic field. Regarding uncertain boundary conditions, in [7] the position of the applied load is considered uncertain. Including the uncertainty on the geometry is anything but trivial. In the literature, one can find different modelling strategies. For example:

- Uncertainty can be integrated indirectly by introducing uncertain hyperparameters, *i.e.*, parameters that are neither design variables nor physical parameters. In this context, in [3], the authors consider the velocity field, which is used to update the geometry in the framework of a level-set algorithm, as uncertain.

- Uncertainty can be integrated directly on the design variables of the TO algorithm. In [5], the authors consider that the design variables, described through geometrical primitives, are affected by uncertainty. In that way, the shape of the primitives are tuned in line with uncertainty.

- Uncertainty can be integrated directly thanks to the finite element mesh, either through the position of the nodes (Lagrangian approach) [9] or on the physical pseudo-density field [15]. The "physical pseudo-density field" is the field of pseudo-density that is used to compute the part metrics. For example, in SIMP (Solid Isotropic Material with Penalisation) penalty scheme, it is the field of pseudo-density that the designer uses to interpret and produce a part. These two modelling strategies offer more compatibility concerning the TO algorithms, since the uncertainty is applied on entities that are independent of the hyperparameters or the design variables.

Of course, this short literature survey is not exhaustive at all. For instance, research works have been conducted on this topic by using the Reliability-Based Design Optimisation (RBDO) [15]. As uncertain sources have been elicited, their characterisation is necessary. Particularly, uncertain variables are characterised either as aleatory or as epistemic; aleatory uncertainty is irreducible, but epistemic uncertainty is reducible if more knowledge is added [14]. Uncertainty Quantification (UQ) for Additive Manufacturing (AM) falls into both representations [13]. This means that TO must be compliant with epistemic uncertainty, even if most works use an aleatory characterisation for uncertainties. Epistemic uncertainty has been taken into account in [7], wherein the uncertainty on load position and thickness of the 2D design space (the thickness is optimised after the use of TO) was represented thanks to intervals, resulting in one robust

geometry. In [12], the angle of the applied force is affected by epistemic uncertainty represented by fuzzy method, the information of this uncertain parameter is integrated in the gradient, resulting in a robust geometry. In [17], material property and load conditions are affected by epistemic uncertainty, they are represented thanks to intervals in a multi-scale context.

Nevertheless, when using such approaches, the designer has only one choice despite the presence of epistemic uncertainty. Generally, this kind of uncertainty is illustrated through a set of Cumulative Distribution Functions (CDFs), where the envelope of these CDFs is referred to as a probability box [14]. Probability box might be used when RBDO method is chosen. In this paper, an adaptation of the standard RTO framework is proposed and applied in order to fit with this representation of epistemic uncertainty to robust design. Moreover, the geometry is considered as uncertain with epistemic uncertainty modelled with Dempster-Shafer or probability boxes (p-boxes) like structures. Of course, this representation is integrated in the classic RTO framework which is adapted accordingly.

The remainder of the paper is organised as follows. Section 2 introduces the model used to describe the geometrical imperfection, by considering the AM process. Then, in Section 3, the formulation of the optimisation problem is detailed, by focusing on the introduction of epistemic uncertainty. In section 4, the obtained results are discussed. Finally, a conclusion is drawn, as well as future work orientations.

2 GEOMETRICAL MODELLING FOR ROBUST TOPOLOGY OPTIMISATION

The proposed geometrical modelling aims at processing local imperfection for AM-like processes. The approach described in this section is limited to TO algorithm using a field of pseudo-density field (projected over the mesh) to describe the topology. When geometrical uncertainties are taken into consideration, the perturbed part can extend beyond the design space, but this aspect is often neglected in the literature. For instance, in [9] perturbation affects both the design and non-design regions of the domain, whereas this aspect is not taken into account in the approach presented in [15]. In the approach presented in this section, uncertainty can affect both design and non-design regions of the definition domain. However, uncertainty can affect only those non-design regions where boundary conditions are not imposed. In the case of an Eulerian mesh, the overall definition domain is discretised by using a mapped mesh composed of hexahedral elements in 3D and quadrilateral elements in 2D. The proposed model takes advantage of this regular discretisation. Moreover, it is noteworthy that Verification and Validation (V&V) procedures for AM and Eulerian meshes are being developed [8]: this fact supports our choice to use models that are compatible with Eulerian meshes.

In the context of density-based TO algorithms, the geometrical imperfections are modelled indirectly by acting on the pseudo-density field. Therefore, the pseudo-density field is affected by uncertainty, and a perturbed pseudo-density field is computed. For all elements i in the overall space, Eq. 1 introduces the geometrical imperfection modelling :

$$\tilde{\rho}_i = \bar{\rho}_i + \Delta\rho_i \ \forall i \in [\![1, N_e]\!] \tag{1}$$

where $\bar{\rho}_i$ is the physical (unperturbed) pseudo-density of the generic element i that belong to the total space, whereas $\tilde{\rho}_i$ is the perturbed counterpart. $\Delta\rho_i$ is the variability (geometric imperfection model) of the pseudo-density of the element i that belongs to the total space and N_e is the number of elements composing the mesh of the FE model.

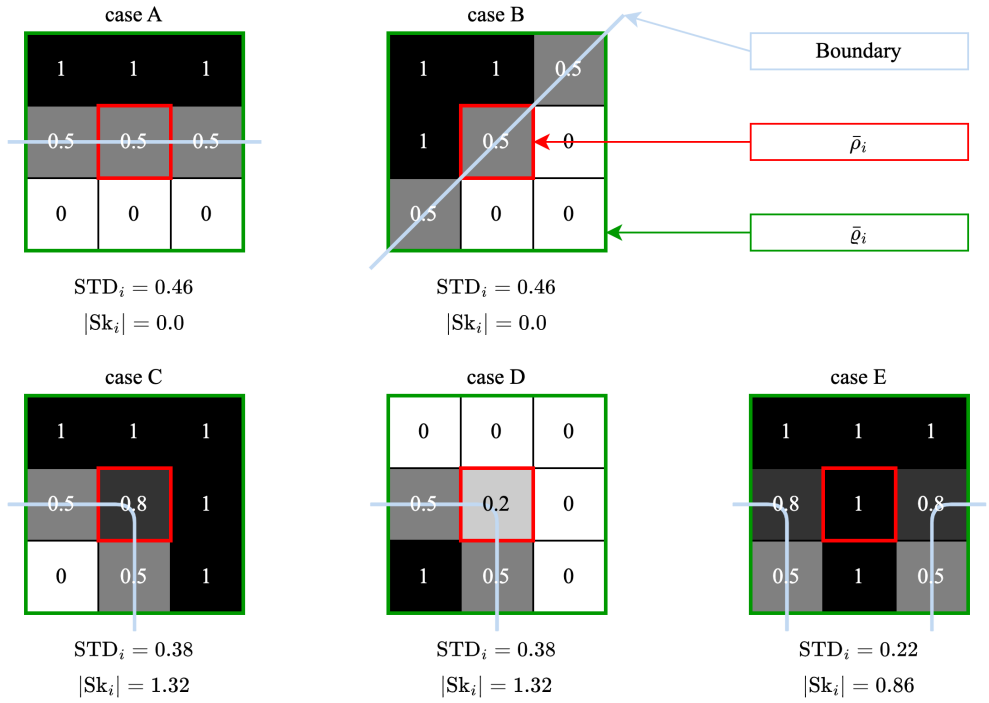

Figure 1: Several boundary configurations and their metrics.

It is noteworthy that the perturbed density field $\tilde{\rho}_i$ can vary in the interval $[0, 1]$, which means that the perturbation $\Delta\rho_i$ is conveniently adjusted when $\bar{\rho} = \rho_{\mathrm{LB}}, \rho_{\mathrm{UB}}$. In other words, all drawn numbers are put back in their physical quantity. Finally, if an element belongs to the non-design region, then $\bar{\rho}_i = 0$ and $\tilde{\rho}_i = \Delta\rho_i$.

The geometric imperfection du to the manufacturing process (with the associated variability) must be integrated inside the variable $\Delta\rho_i$. This variation depends on the process and on local geometric features. In the following, we assume that $\Delta\rho_i$ depends on the neighbourhood of the element i, and only local information of the process is included in $\Delta\rho_i$. For 2D problems, the neighbourhood of the element is defined through a circle of radius r_{loc} and the set containing the indices of the elements falling in this circle is indicated as $\mathcal{S}_i$. The pseudo-densities of the elements falling in the neighbourhood of the element i are denoted as ϱ_j, $j \neq i$, $j \in \mathcal{S}_i$.

In the model of geometrical imperfections, if ϱ_j are close to zero or one $\forall j \in \mathcal{S}_i$, then the probability of a boundary is null. The presence of a boundary (in or close) in $\mathcal{S}_i$ can be characterised by looking at the STandard Deviation (STD) of ϱ_j, as shown in Fig. 1. Moreover, in order to take into account the boundary smoothness, we propose a statistical model, where the boundary curvature is related to the skewness of density of the densities of nth elements belonging to $\mathcal{S}_i$. This aspect is of paramount importance because there is a correlation between curvature of the boundary and geometrical imperfections in AM processes. Figure 1 illustrates various boundary configurations and the values of local skewness and STD for the elements falling in $\mathcal{S}_i$. Cases A and B are characterised by a straight boundary, resulting in a high STD and null skewness. Cases C and D have a fillet radius near the element i, resulting in a smaller STD but higher skewness. In the last case, an element in an arm connection is considered,

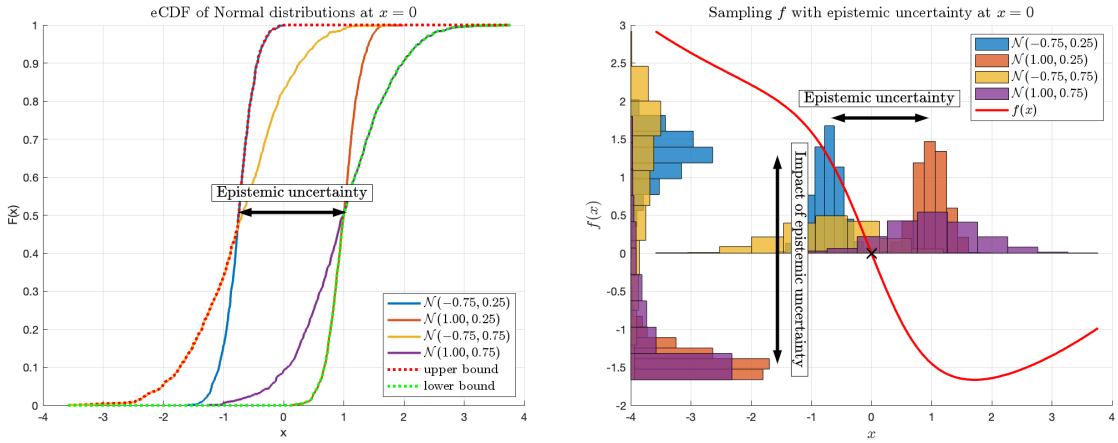

Figure 2: Probability boxes of a normal distribution, on the left; and its repercussion in robust design approach, on the right.

resulting in a smaller STD and skewness. Therefore, the proposed modelling of geometrical imperfections is suited for TO density-based methods and can consider the local curvature of the boundary. Based on the modal decomposition [4], we propose a statistical decomposition of $\Delta\rho_i$ given as follows:

$$\Delta\rho_i = \mathcal{H}\left(\mathrm{STD}\left(\bar{\varrho}_i\right)\right) \times \left(k_{\mathrm{STD}}\mathrm{STD}\left(\bar{\varrho}_i\right) + k_{\mathrm{Sk}}\left|\mathrm{Sk}\left(\bar{\varrho}_i\right)\right|\right) \times \mathcal{X}_{\mathrm{AM}} \tag{2}$$

where $\mathrm{STD}\left(\bar{\varrho}_i\right)$ and $\mathrm{Sk}\left(\bar{\varrho}_i\right)$ are the standard deviation and the skewness of the elements falling in $\mathcal{S}_i$. $\mathcal{X}_{\mathrm{AM}}$ is a random variable associated with the local geometric imperfection (and its distribution) due to the AM process. k_{STD} and k_{Sk} are two model parameters, while $\mathcal{H}\left(x\right) = 1$ if $x > 10^{-4}$ and $\mathcal{H}\left(x\right) = 0$ otherwise.

The next section will discuss the application of Eqs. 1 and 2 in the context of epistemic uncertainty that arise when evaluating $\mathcal{X}_{\mathrm{AM}}$.

3 PROBLEM FORMULATION IN CASE OF EPISTEMIC UNCERTAINTY

3.1 Numerical implementation

Dempster-Shafer and p-boxes structures have the advantage to process epistemic uncertainty and when the distribution is imprecisely specified, this approach is called *direct assumption* [6]. Both structures describe a bounded randomness for a random variable. Instead of having only one distribution, two distributions are defined (lower and upper bounds). It follows that the imprecisely known distribution lies between these two distributions, as shown in the left image in Fig. 2. For Dempster-Shafer structures, the upper bound is denoted as cumulative plausibility function, while the lower bound is indicated as cumulative belief function [6]. Dempster-Shafer and p-boxes structures are interconvertible, even if Dempster-Shafer structures can contain more information [6]. Probability boxes are useful when a probability computation is needed, thus they are better suited for RBDO.

In this article, the random variable $\mathcal{X}_{\mathrm{AM}}$ follows a normal distribution, where its mean is equal to zero and its STD is uncertain and defined on an interval $\sigma_{\mathrm{AM}} = [0.2, 0.6]$. Now, since

$\mathcal{X}_{\mathrm{AM}} \sim \mathcal{N}(0, [0.2, 0.6])$, a p-box is defined and epistemic uncertainty is revealed. In this article, as a RTO method is used, the formulation of the problem needs to be reviewed. In our proposition, two geometries at the end of the optimisation process are generated: an *optimist* geometry and a *pessimist* geometry; helping the designer to make a choice by considering epistemic uncertainty.

TO method used in this work makes use of an element-wise description of the pseudo-density field and it is based on the SIMP penalty scheme. In this background, the robust optimisation problem consists of minimising the mean and the STD of compliance, with a constraint on the volume of the produced geometries: *optimist* (op) and *pessimist* (pe). The optimisation problem is formulated as follows:

$$\begin{aligned} \min_{\boldsymbol{\rho}_{\mathrm{op|pe}}} \hat{\mathcal{C}}\left(\boldsymbol{\rho}_{\mathrm{op|pe}}\right) \quad &= \quad \hat{m}_1\left(\mathcal{C}\left(\tilde{\boldsymbol{\rho}}_{\mathrm{op|pe}}\right)\right) + \sqrt{\hat{\mu}_2\left(\mathcal{C}\left(\tilde{\boldsymbol{\rho}}_{\mathrm{op|pe}}\right)\right)} \\ s.t. \quad & \mathcal{V}\left(\bar{\boldsymbol{\rho}}_{\mathrm{op|pe}}\right) = V^* \\ & \mathbf{f} = \mathbf{K}\mathbf{u} \\ & 0 \leq \rho_i \leq 1 \ \forall i \in [\![1, N_e]\!] \end{aligned} \tag{3}$$

where $\hat{\mathcal{C}}$ is an estimation of a robust metric used for part compliance. $\hat{m}_1$ is a function that gives an estimation of the mean and $\hat{\mu}_2$ is a function that gives an estimation for the variance. $\boldsymbol{\rho}_{\mathrm{op|pe}}$ is the design field, made up of pseudo-densities in SIMP, of the optimist or pessimist geometry. $\bar{\boldsymbol{\rho}}_{\mathrm{op|pe}}$ is the unperturbed (physical) density field of the optimist or pessimist geometry. $\mathcal{C}$ is a function that computes the compliance of a given density field and $\mathcal{V}$ is a function that computes the volume of a given density field, V^* is the desired volume. Finally $\mathbf{u}$, $\mathbf{f}$ and $\mathbf{K}$ are the displacement, force vectors and stiffness matrix, respectively.

According to Eq. 3, two optimisation problems must be solved in order to compute the optimist and pessimist topologies and get, accordingly, bounded results in the same spirit of p-boxes. However, these problems are coupled, in terms of compliance bounds, due to epistemic uncertainty. For a normal distribution, where its standard deviation is described as an interval, two CDFs are needed to define the p-box. One uses the lower bound of the STD interval and the other the upper bound [6]. Unfortunately, non-linearity might affect the estimation of the lower and upper bounds of $\hat{\mathcal{C}}$. As illustrated on the right side of the Fig. 2, the impact of epistemic uncertainty on the system (modelled by a function f in the Fig. 2) might change the bounds order. Particularly, the distributions that describe the bounds are inverted and one almost lies entirely inside the p-box.

Accordingly, a new optimisation workflow needs to be defined for the objective functions estimation. However, to simplify the problem, only some values in the interval are used to compute the lower and upper geometries.

In Eq. 3, the CDF (that can be used to estimate probabilities) is not used as a robust metric. In place of the CDF, the summation of the mean and the STD is used; both are estimated thanks to a Probability Distribution Function (PDF). It is not a problem to define a "lower" and "upper" PDF, as PDFs are derivatives of CDFs, see, for instance the right side of the Fig. 2. In this framework, each PDF is used to update the two geometries, thanks to the estimation of its mean and STD. In fact, in a standard RTO scheme, the mean and the STD are used to compute the gradient and update the geometry thanks to a function, h, that depends on the chosen optimiser:

$$\boldsymbol{\rho}^{j+1} = h\left(\hat{\mathcal{C}}\left(\boldsymbol{\rho}^j\right), \mathcal{V}\left(\boldsymbol{\rho}^j\right) - V^*, \nabla\hat{\mathcal{C}}\left(\boldsymbol{\rho}^j\right), \nabla\mathcal{V}\left(\boldsymbol{\rho}^j\right)\right) \tag{4}$$

where j is the iteration index. The coupling act happens during the update of the two pseudo-density fields. Because the parameters of the probability distribution are sampled, the optimist solution is updated according to this scheme:

$$\boldsymbol{\rho}_{\mathrm{op}}^{j+1} = \underset{\boldsymbol{\rho}_{\mathrm{op|pe}}}{\arg\min} \left\{ \mathcal{C}\left(\boldsymbol{\rho}_{\mathrm{op}}^{j+1}\left(\sigma_{\mathrm{AM}}^{0}\right)\right), \mathcal{C}\left(\boldsymbol{\rho}_{\mathrm{pe}}^{j+1}\left(\sigma_{\mathrm{AM}}^{0}\right)\right), \ldots, \mathcal{C}\left(\boldsymbol{\rho}_{\mathrm{pe}}^{j+1}\left(\sigma_{\mathrm{AM}}^{k}\right)\right) \right\} \tag{5}$$

where k is the length of the sampled values to estimate the p-box like structures or the impact of epistemic uncertainty. Similarly, the pessimist solution update is defined as:

$$\boldsymbol{\rho}_{\mathrm{pe}}^{j+1} = \underset{\boldsymbol{\rho}_{\mathrm{op|pe}}}{\arg\max} \left\{ \mathcal{C}\left(\boldsymbol{\rho}_{\mathrm{op}}^{j+1}\left(\sigma_{\mathrm{AM}}^{0}\right)\right), \mathcal{C}\left(\boldsymbol{\rho}_{\mathrm{pe}}^{j+1}\left(\sigma_{\mathrm{AM}}^{0}\right)\right), \ldots, \mathcal{C}\left(\boldsymbol{\rho}_{\mathrm{pe}}^{j+1}\left(\sigma_{\mathrm{AM}}^{k}\right)\right) \right\} \tag{6}$$

Eqs. 5 and 6 will provide the designer two optimised topologies, which can be seen as the upper and lower bounds of a p-box. Notice that, as stated before, the minimum and maximum of the Eqs. 5 and 6 should be computed by varying the values of the epistemically affected distribution parameters; but here, values are sampled inside an interval. Lastly, the convergence criterion is either based on the maximum number of iterations set by the user or when the following criterion is met:

$$\epsilon = \frac{\left|\hat{\mathcal{C}}\left(\boldsymbol{\rho}_{\mathrm{op}}^{j}\right) - \hat{\mathcal{C}}\left(\boldsymbol{\rho}_{\mathrm{op}}^{j+1}\right)\right|}{\left|\hat{\mathcal{C}}\left(\boldsymbol{\rho}_{\mathrm{op}}^{j}\right)\right| + \left|\hat{\mathcal{C}}\left(\boldsymbol{\rho}_{\mathrm{op}}^{j+1}\right)\right|} + \frac{\left|\hat{\mathcal{C}}\left(\boldsymbol{\rho}_{\mathrm{pe}}^{j}\right) - \hat{\mathcal{C}}\left(\boldsymbol{\rho}_{\mathrm{pe}}^{j+1}\right)\right|}{\left|\hat{\mathcal{C}}\left(\boldsymbol{\rho}_{\mathrm{pe}}^{j}\right)\right| + \left|\hat{\mathcal{C}}\left(\boldsymbol{\rho}_{\mathrm{pe}}^{j+1}\right)\right|} \tag{7}$$

3.2 Sensitivities

Monte Carlo Sampling (MCS) with n samples is used for the estimation of the mean and STD. Given a sample of size n, then it is possible to compute the unbiased moments of the compliance $\mathcal{C}$ and use them in equation 3:

$$\begin{aligned} \hat{m}_1 &= \frac{1}{n}\sum_{l=0}^{n} \mathcal{C}\left(\tilde{\boldsymbol{\rho}}_l\right) \\ \hat{\mu}_2 &= \frac{1}{n-1}\sum_{l=0}^{n} \left(\mathcal{C}\left(\tilde{\boldsymbol{\rho}}_l\right) - \hat{m}_1\right)^2 \end{aligned} \tag{8}$$

where $\tilde{\boldsymbol{\rho}}_l$ is the l^{th} sample from the population. The computation of the sensitivities, for the i^{th} element reads:

$$\begin{aligned} \frac{\partial \hat{m}_1}{\partial \rho_i} &= \frac{1}{n}\sum_{l=0}^{n} \frac{\partial \mathcal{C}\left(\tilde{\boldsymbol{\rho}}_l\right)}{\partial \rho_i} \\ \frac{\partial \hat{\mu}_2}{\partial \rho_i} &= \frac{2}{n(n-1)}\left[n\sum_{l=0}^{n} \left(\mathcal{C}\left(\tilde{\boldsymbol{\rho}}_l\right) - C\right)\frac{\partial \mathcal{C}\left(\tilde{\boldsymbol{\rho}}_l\right)}{\partial \rho_i} - \left(\sum_{l=0}^{n} \left(\mathcal{C}\left(\tilde{\boldsymbol{\rho}}_l\right) - C\right)\right)\left(\sum_{l=0}^{n} \frac{\partial \mathcal{C}\left(\tilde{\boldsymbol{\rho}}_l\right)}{\partial \rho_i}\right)\right] \end{aligned} \tag{9}$$

where the partial derivative of the compliance for the l^{th} sample, *i.e.* $\partial \mathcal{C}\left(\tilde{\boldsymbol{\rho}}\right)/\partial \rho_i$, is already available in the literature (see details in [1] and [10] regarding the expression of the partial derivative of the compliance). It is noteworthy that C is the compliance of the current design (without uncertainty), which is used to reduce the numerical errors when computing the variance and its gradient. This information can be used because the following property holds: $\mathbb{V}\left(X\right) = \mathbb{V}\left(X - C\right)$.

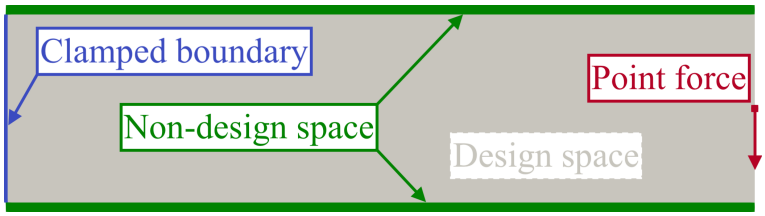

Figure 3: Boundary condition and total space of the study case.

4 NUMERICAL RESULTS

The use case that will be used in this paper is a rectangular design space, with a length to width ratio of 4. The boundary conditions are the following: a downward force in the middle of the right face and fully clamped left face (except on the non-design space). A non-design space is defined at the top and at the bottom of the rectangular design space. The number of elements along the length is 160 and along the height is 40 plus 2 for each non-design space rectangle; as the geometric perturbation is local and depends on the size of the elements, this number is sufficient. Moreover, the side of an element is one. The figure 3 shows the boundary setting.

As the SIMP method is employed, different filters are available in order to: assure mesh independence thanks to the enforcement of a minimal length scale, for this, a filter on the design field is applied by using a moving average on elements that belong to a circle of radius r_{scale}, see details in [1]; and to render the solution black and white, for this, a filter based on a continuous approximation of the Heaviside function is used, see details in [10]. The value of radius for the first filter is $r_{\text{scale}} = 1.3$. For the "Heaviside filter" $\eta = 0.5$ through all the optimisation (an optimal value of η is not calculated at each iteration) and a continuation scheme is applied to the parameter β, its value varies in this vector $[1.0, 4.0, 8.0, 16.0, 32.0, 64.0]$ for this number of iterations $[60, 15, 5, 5, 5, 5]$. The constraint on the volume is set at 40% of material of the design space. Lastly, the SIMP law used in this article is :

$$^{D}(\bar{\boldsymbol{\rho}})/_{D^+} = \alpha + (1-\alpha)\bar{\boldsymbol{\rho}}^p \tag{10}$$

where $\alpha = {}^{D^-}/_{D^+} = 1.10^{-6}$ and D^+ and D^- are the elasticity tensor for full and void materials respectively. The value of the penalty stays at $p = 3$ and no continuation scheme is used.

For the statistical model presented in section 2, the following parameters are used: $k_{\text{STD}} = 1.6$ and $k_{\text{Sk}} = 0.2$; $\mathcal{X}_{\text{AM}} \sim \mathcal{N}(0, [0.2, 0.6])$. A hypothesis is made on the linearity of the framework and only the extremal values are considered, *i.e.* $\sigma_{\text{AM}} = [0.2, 0.6]$; $r_{\text{loc}} = 1.5$, which means, by considering the size of an element, the configuration is similar to the ones shown in figure 1; and the sample size for the MCS is $n = 1000$.

Finally, for the optimiser, the routine update function, h, used is the one that came from this article [1]; even though, the MMA optimiser from NLopt can be used, but the comparison between different optimisers is planned for a future paper. For the chosen optimiser, the tolerance for the volume constraint is 0.001 and the "move" variable is 0.2. All the code is running with Python 3.10; finite element simulations, for the linear elasticity problem, are made with DOLFINx [2] and the mesh with Gmsh.

The figure 4 depicts the geometry obtained without uncertainties. The compliance is about 397 and the shape is classic for this kind of problem setting. It can be observed that the addition of a non-design space has no influence on the result. The figure 5 represents the geometries

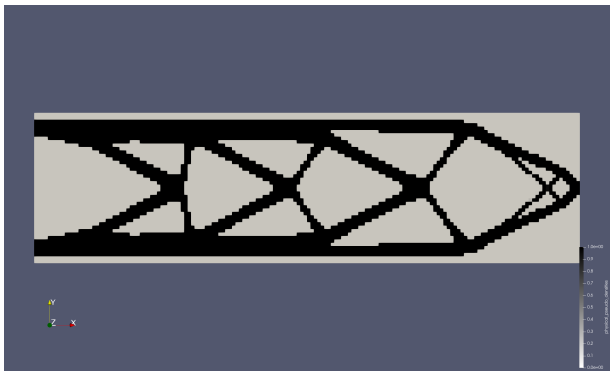

Figure 4: Optimised geometry obtained without uncertainty.

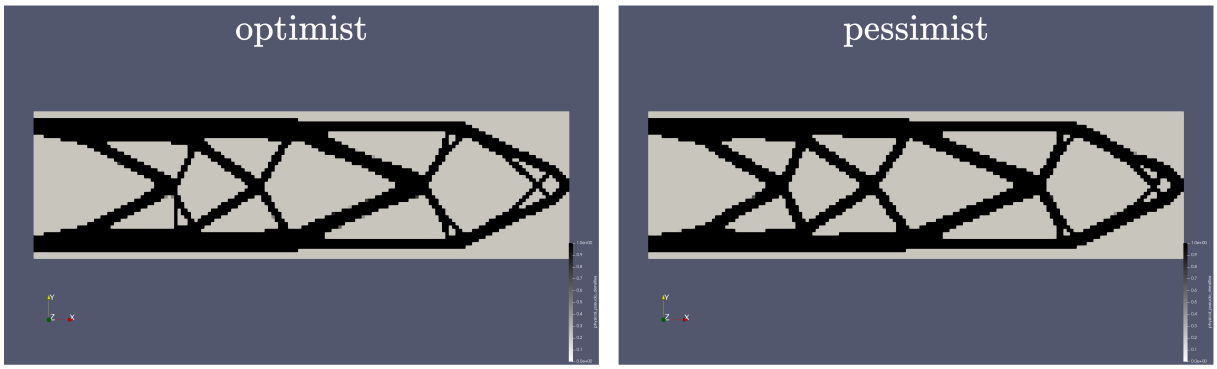

Figure 5: Optimised geometries affected by uncertainties, on the left: the optimist geometry ; on the right: the pessimist geometry.

obtained with epistemic uncertainty. Has mentioned previously, two geometries results from this new optimisation process. The optimist geometry on the left of figure 5 and the pessimist geometry on the right of figure 5. The table 1 sum-up the main metrics for all the geometries. Regarding cases with uncertainty, the mean and the STD are higher for the pessimist geometry as intended. The standard deviation is relatively small, which is consistent as the uncertainty model is local. The shapes became thicker if the geometric uncertainty is considered and the optimiser succeeded to distribute the material according to the levels of uncertainty. When uncertainty is considered, shapes lose their symmetries, it is due to the sampling method; if the number of individuals in the population is increased, then the shapes are more symmetric. As the designer has more information on the relative shape that is produced by different levels of uncertainty and as the shape is similar; it can help to know where to increase arm size. Finally, the fact that the geometries look similar, with more or less thick arms is not a general conclusion; precautions should be taken and further investigation needs to be made.

5 CONCLUSION

In this article process information is integrated thanks to DFR activity. A questioning on the type and on the representation of uncertainties was asked. It follows that both, epistemic and

Table 1: Comparison on different metrics between geometries.

	Compliance	Mean	STD	Max.	Min.
No uncertainty	397	N/A	N/A	N/A	N/A
Optimist	400	449	2.86	460	442
Pessimist	413	463	3.11	474	453

aleatory, uncertainty can emanate from the process. That is why, an adaptation of the classic RTO framework is proposed and applied compared to the p-boxes that are found in RBDO. In this framework, two geometries are produced at the end of the optimisation, in the spirit of the classical p-boxes. The results are cohesive with what is expected. The optimist geometry has a better performance in compliance, but result in a slender design.

The future steps of this work are to verify the hypothesis on the linearity of the framework. Moreover, other optimisers can be used and other use cases are required to see if the three geometries will stay similar. Finally, this work, can be extended to textbook cases of the robust design community to have a deeper look inside the method fulfilled in this paper.

ACKNOWLEDGEMENTS

This paper has been supported by the Agence National de la Recherche (ANR) for the project Robust Design For Additive Manufacturing (RobustAM) under the following reference ANR-21-CE10-0005, which is thankfully acknowledged by the authors. Moreover the authors want to express their gratitude to the open source community.

REFERENCES

[1] E. Andreassen, A. Clausen, M. Schevenels, B. S. Lazarov, and O. Sigmund. Efficient topology optimization in matlab using 88 lines of code. *Structural and Multidisciplinary Optimization*, 43(1):1–16, 2011.

[2] I. A. Baratta, J. P. Dean, J. S. Dokken, M. Habera, J. S. Hale, C. N. Richardson, M. E. Rognes, M. W. Scroggs, N. Sime, and G. N. Wells. DOLFINx: the next generation FEniCS problem solving environment. preprint, 2023.

[3] S. Chen and W. Chen. A new level-set based approach to shape and topology optimization under geometric uncertainty. *Structural and Multidisciplinary Optimization*, 44(1):1–18, 2011.

[4] J.-Y. Dantan, Z. Huang, E. Goka, L. Homri, A. Etienne, N. Bonnet, and M. Rivette. Geometrical variations management for additive manufactured product. *CIRP Annals*, 66(1):161–164, 2017.

[5] S. De, J. Hampton, K. Maute, and A. Doostan. Topology optimization under uncertainty using a stochastic gradient-based approach. *Structural and Multidisciplinary Optimization*, 62(5):2255–2278, 2020.

[6] S. Ferson, V. Kreinovick, L. Ginzburg, and F. Sentz. Constructing probability boxes and dempster-shafer structures. Technical report, Sandia National Lab.(SNL-NM), Albuquerque, NM (United States); Sandia, 2003.

[7] S. Freitag, S. Peters, P. Edler, and G. Meschke. Reliability-based optimization of structural topologies using artificial neural networks. *Probabilistic Engineering Mechanics*, page 103356, 2022.

[8] R. M. Gorguluarslan, R. V. Grandhi, H.-J. Choi, and S.-K. Choi. Prediction assessment and validation of multiscale models for additively manufactured lattice structures under uncertainty. *Journal of Mechanical Science and Technology*, 33(3):1365–1379, 2019.

[9] M. Jansen, G. Lombaert, and M. Schevenels. Robust topology optimization of structures with imperfect geometry based on geometric nonlinear analysis. *Computer Methods in Applied Mechanics and Engineering*, 285:452–467, 2015.

[10] B. S. Lazarov, M. Schevenels, and O. Sigmund. Robust design of large-displacement compliant mechanisms. *Mechanical Sciences*, 2(2):175–182, 2011.

[11] B. S. Lazarov, M. Schevenels, and O. Sigmund. Topology optimization considering material and geometric uncertainties using stochastic collocation methods. *Structural and Multidisciplinary Optimization*, 46(4):597–612, 2012.

[12] Z. Meng, Y. Wu, X. Wang, S. Ren, and B. Yu. Robust topology optimization methodology for continuum structures under probabilistic and fuzzy uncertainties. *International Journal for Numerical Methods in Engineering*, 122(8):2095–2111, 2021.

[13] P. Nath, J. D. Olson, S. Mahadevan, and Y.-T. T. Lee. Optimization of fused filament fabrication process parameters under uncertainty to maximize part geometry accuracy. *Additive Manufacturing*, 35:101331, 2020.

[14] C. J. Roy and W. L. Oberkampf. A comprehensive framework for verification, validation, and uncertainty quantification in scientific computing. *Computer Methods in Applied Mechanics and Engineering*, 200(25):2131–2144, 2011.

[15] Y. Sato, K. Izui, T. Yamada, S. Nishiwaki, M. Ito, and N. Kogiso. Reliability-based topology optimization under shape uncertainty modeled in eulerian description. *Structural and Multidisciplinary Optimization*, 59(1):75–91, 2019.

[16] G. Schuëller and H. Jensen. Computational methods in optimization considering uncertainties – an overview. *Computer Methods in Applied Mechanics and Engineering*, 198(1):2–13, 2008. Computational Methods in Optimization Considering Uncertainties.

[17] L. Wang, Y. Cai, and D. Liu. Multiscale reliability-based topology optimization methodology for truss-like microstructures with unknown-but-bounded uncertainties. *Computer Methods in Applied Mechanics and Engineering*, 339:358–388, 2018.

[18] L. Zhou, O. Sigmund, and W. Zhang. Self-supporting structure design with feature-driven optimization approach for additive manufacturing. *Computer Methods in Applied Mechanics and Engineering*, 386:114110, 2021.